Asian Journal of Civil Engineering (2023) 24:1181–1198
https://doi.org/10.1007/s42107-022-00561-6

RESEARCH

Free vibration analysis of laminated composite porous plate

Raushan Kumar[1] · **Ajay Kumar**[2]

Received: 16 November 2022 / Accepted: 28 December 2022 / Published online: 24 January 2023

Abstract
In the present work, the free vibration response of laminated composite porous plates explored using improved cubic shear deformation theory. It is the first attempt to analyse vibration analysis of the laminate using this advanced theory. In this theory, transverse shear stress continuity incorporated at the interface of each laminate in conjunction with free surface consideration at the plate top and bottom. The different types of porosity distribution introduced in the entire thickness of the plate. A 2D finite element model developed for the present mathematical model to analyse the fundamental frequency of the porous plate. Due to the interface shear stress continuity of individual layers, the improved third-order shear deformation theory depicts better results than the first, second, and third-order theories. An in-house FORTRAN code developed for the present study by the authors. The effects of different orientation angles, boundary conditions, and material properties on the fundamental frequency were investigated with different numerical examples. The convergence study was conducted to determine the stability and accuracy of the present model. The results in comparison with the literature found to agree well.

Keywords Free vibration · Porous plate · Finite element · Laminated plate · Numerical example

Introduction

Recent studies have focused on the vibrations of multi-layered composite plates. Use of this research is for the marine system, laminated construction, aircraft, etc. Hence, it increased the interest of engineers while modelling such structures under the effects of dynamic behaviour, leading to an exact solution and saving computational time. Many researchers have done work related to the vibration analysis of isotropic and composite plates. It can be seen in detail in the literature. Nosier et al. (1993) performed Reddy's research using layer-wise theory to determine natural frequency and various mode shapes and elasticity equations are explained with the help of state-space variables and transfer matrix. Qatu (1994) presented known natural frequency for different shapes of a cross-section of cantilever laminated angle ply, such as triangular, trapezoidal, and so on, and also analysed for convergence and obtained reasonably accurate results. Cheung and Zhou (2001) investigated free vibration due to static sinusoidal loading of rectangular laminated plates. In this investigation vibrating trial function is used in this study for the in-plane shear deformation of the plate. Shimpi (2002) performed a single response of bending and shear i.e., not contributed to each other by using loading bending moment and shear forces. The effectiveness of this theory is performed by numerical examples. Liew (2003) computed natural frequency due to the vibration effect of the laminated plate and compare it with the published result using moving least square deferential quadrilateral methods. Jianwei et al. (2004) analysed a simply supported curve panel with the help of higher-order shear deformation theory. A set of Fourier series function is formed for the highly coupled deferential equation and the boundary conditions. Ferreira and Fasshauer (2006) performed a numerical result and discussed different thickness-to-length ratios for the vibration analysis of the Timoshenko beam. Magnucka-Blandzi and Magnucki (2007) derived a differential equation of equilibrium on the basis of minimum potential energy for designing a sandwich beam having metal core foam. Liu et al. (2008) used the linearly interpolation method a mesh-free approach is made for the flexure analysis of the

✉ Ajay Kumar
sajaydce@gmail.com

Raushan Kumar
raushanmit2k8@gmail.com

[1] Department of Civil Engineering, National Institute of Technology Patna, Patna 80005, India

[2] Department of Civil Engineering, National Institute of Technology Delhi, Delhi 110036, India

multi-layered combined beam. Seçgin and Sarigül (2008) presented the first computer algorithm then it verifies with the discrete solution convolution for the exact simply supported thin beam having simply supported end condition. Zhang et al. (2008) investigated using Bernoulli's-Euler flexural hypothesis due to load for the dynamic responses to the double-beam connected elastically having simply supported end condition. Ferreira et al. (2011) performed using a radial-based formulation to the buckling and dynamic responses of isotropic layered plates, and a numerical approach is explained for the same. Benachour et al. (2011) presented that the refined lamina method for the transverse stress causes a parabolic distribution of shear strain without shear correction for the vibration analysis having different gradient values. Palmeri and Adhikari (2011) investigated the vibration analysis of a double-beam system with an elastically connected outer beam and an inner viscoelastic beam, and a numerical example was performed to ensure the accuracy of the results. Bîrsan et al. (2012) examined the direct approach for the deformation analysis of a functionally graded beam. It is performed in general analytical formulation and it is valid for any shape of cross-section. Qu et al. (2013) performed with different boundary conditions of vibration behaviour of a shell using the first shear deformation hypothesis. Material properties are varied to the thickness of the shell. Bhardwaj et al. (2015) developed a finite element model having eight nodded triangular cut-out and analysed it with the help of ANSYS Code. A convergence study is also conducted for available literature and then analysed for varying edge conditions, material characteristics, thickness ratio and geometry of the cut-out. Li et al. (2016) performed a semi-numerical hypothesis to determine the dynamic responses of a double-beam approach with the viscoelasticity of the inside layer of the plate. Based on frequency and mode shape, a nodal-expansion approach is further applied to analyse the response of forced vibration. Li and Sun (2016) analysed the natural frequency and mode shape with the help of a semi-analytical hypothesis for the double-beam approach having a uniformly distributed elastic layer with arbitrary boundary condition, material properties, thickness ratio and loading condition. Rezaei and Saidi (2016) observed that due to the change in porosity effect along the thickness of the plates, changes the mechanical properties of the laminated rectangular cellular plates. It follows the cosine rule for properties of the cellular plate and observes that natural frequency is decreased by the porosity effect in each discussed boundary condition. Belarbi et al. (2017) investigated with analytical approach and analysed it by higher order layered theory for the flexural analysis of the multi-layered plate. Gurjar et al. (2017) examined an orthotropic laminated plate for dynamic responses of a symmetric thick plate using an ANSYS design language for the finite element model using first-order shear deformation hypothesis. Rezaei et al. (2017) examined the dynamic behaviour of a laminated plate with two boundary layer functions. The effect of changes in porosity, thickness ratio, material properties, and aspect ratio on natural frequency appears to be investigated in depth. Ebrahimi et al. (2017) investigated dynamic responses due to magneto electric elasticity laminated plate having even and uneven porosity by analytical methods for the arbitrary boundary condition. It seems that mechanical properties vary with plate thickness, and porosity distribution approximates a power law. Muni Rami Reddy et al. (2018) investigated dynamic responses of thin and thick layered plates with the help of an analytical approach and found all possible natural frequencies of the plate. Arshid and Khorshidvand (2018) examined the dynamic behaviour of porous curved plates with piezoelectric patches. Researchers consider thin plates and transverse shear stress to be neglected. The methodology has been made with the help of classical plate theory. Wang's et al. (2019) proposed a two-dimensional elasticity model by assuming plane stress in each layer of the laminate and edge conditions are linked with the 2D elasticity hypothesis. Saidi and Sahla (2019) presented a new deformation theory of the natural frequency with the elasticity medium of a porous plate. In this study, a new porosity distribution is introduced for the formation of porosity during the fabrication of the functionally graded plate inside. Safaei et al. (2019) examined the fundamental response of various plate models, including the higher deformation theory and plate theory of carbon nanotube-containing plates. The material properties of nanocarbon tubes are investigated using a multiscale finite element approach for different composites. It analysed the porosity effect of multi-layered plate based on higher-order theory and parabolic distribution of stress is experienced along the thickness of the plate and due to shear correction is neglected. Merdaci (2019) analysed the porosity effect of a layered plate using higher order deformation hypothesis, and a nonlinear distribution of stress is experienced to the plate thickness and due to this shear correction is neglected. With isogeometric analysis, Xue et al. (2019) investigated porosity effect of thick plates having different types of cross-section such as circular, rectangular, and square. He presented numerical examples with different porosity distribution, boundary condition and material properties for validation of results. Ghasemi and Meskini (2019) performed a circular cylindrical shell with a porosity effect with the help of Love's shell hypothesis and found that with an increase in porosity coefficient, the non-dimensional frequency decreases. Yüksel and Akbaş (2019) considered a uniform porosity model for the laminates and material properties are orthotropic and a computer programme is used for the result computation. In the analytical approach, the porosity distribution, orientation and sequence of the laminate are investigated, and it is found that porosity is a significant

change to the free vibration analysis of laminated plates. Alambeigi et al. (2020) presented three arbitrary models for porosity that were introduced for theforce and free vibration of the plate. The porosity distribution is along the thickness of the core and the result is validated with different literature. A mathematical model investigated by Soleimanian et al. (2020) of the perforated composite plate for the vibrational analysis due to the temperature effect. Based on the classical plate hypothesis, a significant change in the result has been found due to perforation for the thermal buckling and vibrational frequency. Belarbi et al. (2021) investigated a layer-wise model for the vibrational analysis of sandwich plates for different boundary conditions. The advantage of this study is that when varying the number of layers on the plate, unknowns may be fixed and the results are compared for 2D, 3D quasi, and 3D convergence studies, which are beneficial for both thin and thick layered sandwich plates. Many studies have been conducted by researchers for rectangular, square, and circular laminated plates, with less attention being paid to the elliptical shape, but Balak et al. (2021) studied the vibrational behaviour of a porous-core elliptical lamina having two piezoelectric layers. Adopted theory is widely used for a variety of boundary conditions, including simple and fixed, and getting better results for frequency. Kim et al. (2021a, 2021b) performed a double beam system for vibrational analysis of functionally graded plates. The correctness and convergence of the applied methods are satisfied by having different literature using a finite element approach. A lot of new results have been found for the frequency characteristics of the plate. Zhang et al. (2021) introduced a mathematical model for double beam systems for fundamental frequency of multi-layered 3D plate. Now a combination of first-order deformation theory and classical plate theory are introduced in the governing equation. In addition to it Fourier series is also applied to the mathematical model in order to find natural frequency and mode shape with complex boundary conditions. Devarajan (2021) investigated the effects of iso-geometric vibration on the curvilinear plate using first-order shear deformation. The convergence study is carried out and the new result is analysed with numerical examples with different angles of orientation, thickness ratio, sequence of laminate, shape and boundary condition of laminate. Kim et al. (2021a, 2021b) introduced the elastic sprig technique for different boundary conditions for the dynamic responses of the double plate system plate. By using meshfree discussion, all displacement functions are considered, including boundary condition. The proposed model is validated with past literature and analytical methods. A detailed discussion of the fundamental frequency is to be done in the present study for the different shapes of boundary conditions and material properties. Kumar et al. (2021) investigated a varying depth porous functionally graded plate for normal frequency, which was resting on Pasternack's and Winkler's elastic foundation system. The numerical solution is presented with varying, height-to-width ratio, support conditions, and shape of the layered plate. Verma et al. (2022) investigated carbon boron-based matrixes for the normal frequency of the lamina using classical plate theory for different support conditions. Sayyad et al. (2022) analysed the circular beam for dynamic responses and static analysis with even and uneven porosity due to a lack of literature. A numerical example is discussed for the non-dimensional values of displacement stresses and fundamental frequency having different even and uneven porosity, power law index, and radius of curvature. Van Vinh and Huy (2022) presented analytical methods for the flexural, buckling, and nonlinear responses of the porous plate using the hyperbolic shear deformation hypothesis. With the help of computer code in MATLAB, he analysed the mechanical behaviour of the multi-layered plate with different porosity distributions and the significant role of porosity is discussed with a numerical problem in detail. In this research article, entire analysis is due to the porosity effect, different orientation angle and different edge condition had been analysed for the dynamic response of the multi-layered plate. Many researchers had been used methods like first, second and third-order theory in the past year. No one Researcher has used improved third-order theory as method for free vibration analysis for the laminated porous plate. All results are computed based on improved third-order theory. I analysed various example for the normalized fundamental frequency with help of In-house code with a 2D finite element model.

Methodology

Free vibration analysis and governing equation

The present study consists of free vibration analysis and governing equation for this analysis is as follows:

$$[K]\{\varphi\} = \omega^2[M]\{\varphi\} \tag{1}$$

Stress–strain relationship

In Fig. 1 a four-layered rectangular plate has been shown which has length are L_X and L_Y. The thickness is shown in Z direction. The plate is split into three equal sections with symmetry about the midplane. So that individual thickness of the plate is h/6 and h/3 is in the upper part and same thickness in the lower part of the plate. In the present investigation, three different lamina are opted with different orientation angle having simply supported edge condition. The whole segment of the laminate illustrated in Fig. 2, uses

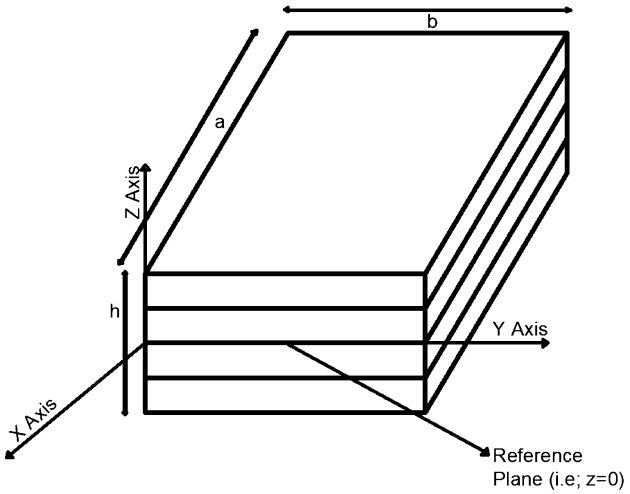

Fig. 1 Four-layered simply supported plate

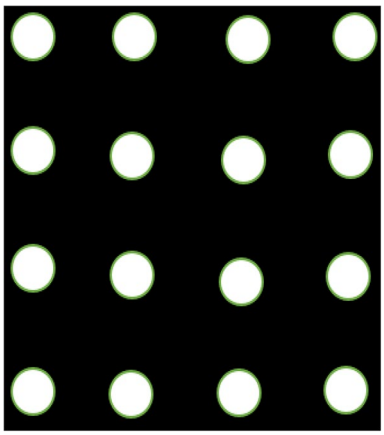

Fig. 2 Distribution of porosity

the porosity distribution model. This distribution approach states that the material characteristics for the laminate (E) vary depending on the young modulus, poison's ratio, etc., and are followed as $E(p)=E(1\text{-}p)$. Below is a detailed discussion of the relation between stress and strain:

$$\begin{Bmatrix}\sigma_x\\ \sigma_y\\ \tau_{xy}\\ \tau_{xz}\\ \tau_{yz}\end{Bmatrix}=\begin{bmatrix}\overline{Q}_{11}(p) & \overline{Q}_{12}(p) & \overline{Q}_{16}(p) & 0 & 0\\ \overline{Q}_{12}(p) & \overline{Q}_{22}(p) & \overline{Q}_{26}(p) & 0 & 0\\ \overline{Q}_{16}(p) & \overline{Q}_{26}(p) & \overline{Q}_{66}(p) & 0 & 0\\ 0 & 0 & 0 & \overline{Q}_{55}(p) & \overline{Q}_{45}(p)\\ 0 & 0 & 0 & \overline{Q}_{45}(p) & \overline{Q}_{44}(p)\end{bmatrix}\begin{Bmatrix}\varepsilon_x\\ \varepsilon_y\\ \gamma_{xy}\\ \gamma_{xz}\\ \gamma_{yz}\end{Bmatrix} \quad \text{or} \quad \{\overline{\sigma}\}=\left[Q^{-i}\right]\{\overline{\varepsilon}\} \tag{2}$$

Here the materials' characteristics (E_1, E_2, ν_{12},G_{13} ,G_{23}, G_{12}) and the angle of orientation (θ), Which is used to developed for the rigidity matrix $\left[Q^{-i}\right]$ in the present study.

$$\begin{aligned}
\overline{Q}_{11}(p) =& Q_{11}(p)\cos^4\theta + 2(Q_{12}(p) \\
&+ 2Q_{66}(p))\sin^2\theta\cos^2\theta + Q_{22}(p)\sin^4\theta \\
\overline{Q}_{12}(p) =& (Q_{11}(p) + Q_{22}(p) - 4Q_{66}(p))\sin^2\theta\cos^2\theta \\
&+ Q_{12}(p)(\cos^4\theta + \sin^4\theta) \\
\overline{Q}_{22}(p) =& (Q_{22}(p)\cos^4\theta + 2(Q_{12}(p) + 2Q_{66}(p))\sin^2\theta\cos^2\theta \\
&+ Q_{11}(p)\sin^4\theta) \\
\overline{Q}_{16}(p) =& (Q_{11}(p) - Q_{12}(p) - 2Q_{66}(p))\sin\theta\cos^3\theta \\
&+ (Q_{12}(p) - Q_{22}(p) + 2Q_{66}(p))\sin^3\theta\cos\theta \\
\overline{Q}_{26}(p) =& (Q_{11}(p) - Q_{12}(p) - 2Q_{66}(p))\sin^3\theta\cos\theta \\
&+ (Q_{12}(p) - Q_{22}(p) + 2Q_{66}(p))\sin\theta\cos^3\theta \\
\overline{Q}_{66}(p) =& (Q_{11}(p) + Q_{22}(p) - 2Q_{12}(p) \\
&- 2Q_{66}(p))\sin^2\theta\cos^2\theta + \overline{Q}_{66}(p)(\cos^4\theta + \sin^4\theta)
\end{aligned}$$

$$\begin{aligned}
\overline{Q}_{44}(p) &= G_{13}(p)\cos^2\theta + G_{23}(p)\sin^2\theta \\
\overline{Q}_{45}(p) &= (G_{13}(p) - G_{23}(p))\sin\theta\cos\theta \\
\overline{Q}_{55}(p) &= G_{23}(p)\cos^2\theta + G_{13}(p)\sin^2\theta
\end{aligned},$$

$$\begin{aligned}
Q_{11}(p) =& \frac{E_1(p)}{1-\nu_{12}(p)\nu_{21}(p)}, Q_{12} = \frac{\nu_{12}(p)E_2(p)}{1-\nu_{12}(p)\nu_{21}(p)}, \\
& Q_{22} = \frac{E_1(p)}{1-\nu_{12}(p)\nu_{21}(p)}, Q_{66} = G_{12}(p).
\end{aligned} \tag{3}$$

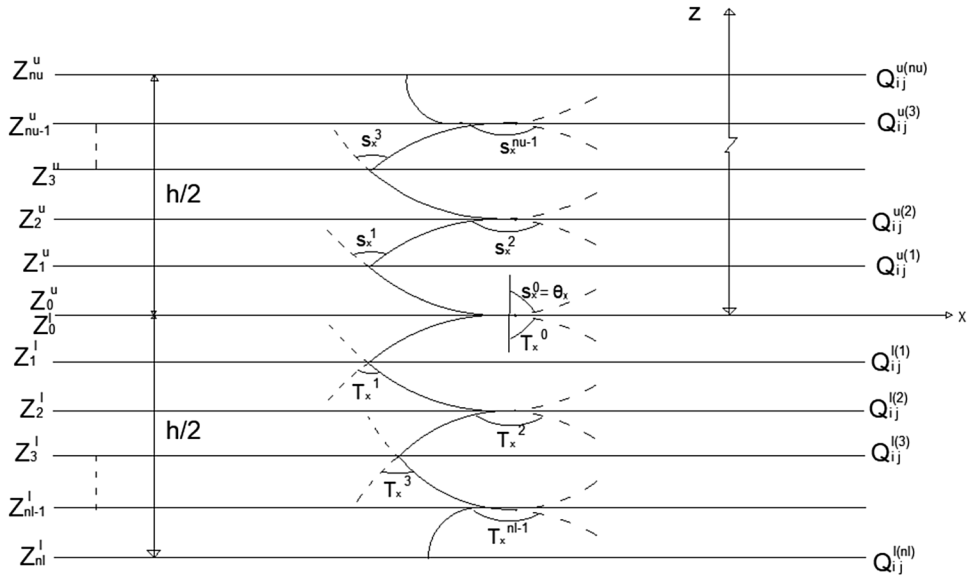

Fig. 3 In-plane displacement throughout the laminate's plate thickness

Relationship between material characteristics and displacement

In Fig. 3, the variation of in-plane displacement over the plate's thickness at the interfaces of the several laminated layers is displayed.

$$\begin{aligned}\{u_1\} =& \{u_1^0\} + \sum_{i=0}^{nu-1} S_1^i (Z - Z_i)\{H\}(Z - Z_i) \\ &+ \sum_{i=1}^{nl-1} T_1^i (Z - \rho_i)\{H\}(-Z + \rho_i) \\ &+ \{\xi_1\} Z^2 + \{\varphi_1\} Z^3 \end{aligned} \tag{4}$$

$$\begin{aligned}\{u_2\} =& \{u_2^0\} + \sum_{i=0}^{nu-1} S_2^i (Z - Z_i)\{H\}(Z - Z_i) \\ &+ \sum_{i=1}^{nl-1} T_2^i (Z - \rho_i)\{H\}(-Z + \rho_i) \\ &+ \{\xi_2\} Z^2 + \{\varphi_2\} Z^3 \end{aligned} \tag{5}$$

where *nu* and *nl* stand for the number of the upper layer and lower layer, respectively, and $\{u_1^0\}$ indicate the in-plane displacement for any point to the middle layer surface.S_1^i, S_2^i, T_1^i, T_2^i represent the gradient of *i*th layer of the lower and upper layers, respectively. Unit step functions, higher-order unknown terms, and coordinate directions are represented by $\{H\}(Z - Z_i)$, $(Z - \rho_i)$,$\{\xi_1\}$, $\{\xi_1\}$, $\{\varphi_1\}$, $\{\varphi_2\}$, and 1, 2 (i.e., x, y in this equations), respectively.

Transverse displacement is considered to be constant over the full thickness of the plate. which is a function of x and y i.e.,

$$\{u_3\} = \{w\} \tag{6}$$

By excluding some terms from HZT's in-plane displacement expressions, FSDT and Third order theory were substituted for the expansion-enhanced higher-order theory. By excluding the following terms from Eqs. 4 and 5, Zig zag theory becomes the important generic hypothesis. For higher-order shear deformation theory, all not included S_1^i, S_2^i,S_3^i, T_1^i, T_2^i,T_3^i exceptS_1^0, $T_{1,}^0 S_{2,}^0$, T_2^0, S_3^0, T_3^0 and for FSDT expecting ξ_i, φ_i and all S_α^i, T_α^i, except S_α^0, T_α^0, where $\alpha = 1,2$ i.e., x and y direction of the laminated plate.

Using the edge condition and transverse shear stress for the top and bottom of the plate. $\sigma_{3\alpha/z=\pm h/2} = 0$ now ξ_α and φ_α of the advanced third-order shear deformation hypothesis may be presented, where $\alpha = 1, 2$ represent x and y coordinate of the laminated plate

$$\{\varphi_1\} = -\frac{4}{3h^2}\left\{ w_1 + \frac{1}{2}\left(\sum_{i=0}^{nu-1} S_1^i + \sum_{i=0}^{nl-1} T_1^i \right) \right\} \tag{7}$$

$$\{\varphi_2\} = -\frac{4}{3h^2}\left\{ w_2 + \frac{1}{2}\left(\sum_{i=0}^{nu-1} S_2^i + \sum_{i=0}^{nl-1} T_2^i \right) \right\} \tag{8}$$

$$\{\xi_1\} = -\frac{1}{2h}\left\{ w_1 + \frac{1}{2}\left(\sum_{i=0}^{nu-1} S_1^i - \sum_{i=0}^{nl-1} T_1^i \right) \right\} \tag{9}$$

$$\{\xi_2\} = -\frac{1}{2h}\left\{ w_2 + \frac{1}{2}\left(\sum_{i=0}^{nu-1} S_2^i - \sum_{i=0}^{nl-1} T_2^i \right) \right\} \tag{10}$$

Comparatively, by substituting the continuation of the transverse stress to the inner layer of surfaces. The subsequent $S_\alpha and\, T_\alpha$ expressions are mentioned as follows:

$$S_1^i = a_{1\gamma}^i \left(w_\gamma + \Psi_\gamma \right) + b_{1\gamma}^i w_{,\gamma} \tag{11}$$

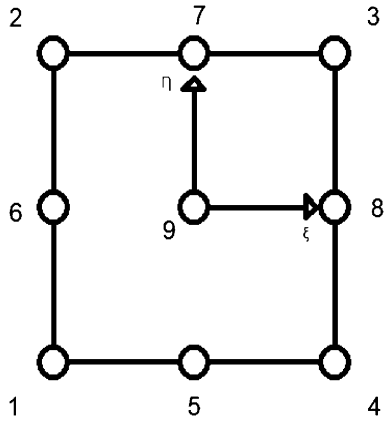

Fig. 4 Nine nodded isoparametric element

$$S_2^i = a_{2\gamma}^i\left(w_\gamma + \Psi_\gamma\right) + b_{2\gamma}^i w_{,\gamma} \tag{12}$$

$$T_1^i = c_{1\gamma}^i\left(w_\gamma + \Psi_\gamma\right) + d_{1\gamma}^i w_{,\gamma} \tag{13}$$

$$T_2^i = c_{2\gamma}^i\left(w_\gamma + \Psi_\gamma\right) + d_{2\gamma}^i w_{,\gamma} \tag{14}$$

where $a_{1\gamma}^i, b_{1\gamma}^i, a_{2\gamma}^i, b_{2\gamma}^i, c_{1\gamma}^i, d_{1\gamma}^i, c_{2\gamma}^i, d_{2\gamma}^i$ are constants, which depends on the material characteristics and geometry of each layers and $w_{,\gamma}$ is a transverse displacement derivative which is assumed as constant earlier, where γ=1, 2 and $S_\alpha^0 = \Psi_\alpha$ is angular displacement about midpoint of the axis where. Now by using Eq. (2), Eqs. (4) and (5)–Eqs. (13) and (14) we find strain field vector and it is obtained as:

$$\left\{\bar{\varepsilon}\right\} = [H]\{\varepsilon\} \tag{15}$$

$\{\varepsilon\}$ is corrected midplane strain, which has a size of 17×1, and $\left\{\bar{\varepsilon}\right\}$ is the strain field vector of matrix size 5×1. $[H]$ matrix having size of 5×17 comprises relevant term to material characteristics and 'z' containing terms

$$\{\varepsilon\}^T = \left\{\begin{array}{l} \frac{\delta u_1}{\delta x}\frac{\delta u_2}{\delta y}\frac{\delta u_2}{\delta x} + \frac{\delta u_1}{\delta y}\frac{\delta w_1}{\delta x}\frac{\delta w_2}{\delta y}\frac{\delta w_2}{\delta x}\frac{\delta w_1}{\delta y}\frac{\delta \psi_1}{\delta x}\frac{\delta \psi_2}{\delta y} \\ \frac{\delta \psi_2}{\delta x}\frac{\delta \psi_1}{\delta y}\Psi_1\Psi_2\frac{\delta w}{\delta x}\frac{\delta w}{\delta y}w_1 w_2 \end{array}\right\} \tag{16}$$

$$\{\varepsilon\} = [B]\{\delta\} \tag{17}$$

where $\{\delta\}$ is the unknown nodal vector having a matrix size of 63×1. $[B]$ is the usual strain displacement matrix having a size of 17×63.

Finite element formulation

The displacement fields must have C^1 continuity with the transverse displacement to use the finite element formulation. The derivatives of w are written as to avoid issues with C^1 continuity with respect to x and y are written as

$$\frac{\delta w}{\delta x} = w_1 \quad \text{and} \quad \frac{\delta w}{\delta y} = w_2 \tag{18}$$

The aforementioned equations aid in defining all changeable terms, including w_1 and w_2 as C^0 continuity. The nine nodded quadrilateral C^0 continuous isoperimetric element employed in the current study has seven degrees of node freedom and is mentioned below. Figure 4 illustrate an isoparametric element with nine nodes.

$$u_1 = \sum_{i=1}^{9} N_i u_i,\ u_2 = \sum_{i=1}^{9} N_i v_i,\ u_3 = \sum_{i=1}^{9} N_i u_i,\ \psi_1 = \sum_{i=1}^{9} N_i \psi_{1i},$$
$$\psi_2 = \sum_{i=1}^{9} N_i \psi_{2i},\ w_1 = \sum_{i=1}^{9} N_i w_{1i},\ w_2 = \sum_{i=1}^{9} N_i w_{2i} \tag{19}$$

where N_i is the shape function of the i_{th} node and shape function for analysis of the model is given below:

$$N_1 = (1-\xi)(1-\eta)/4;\ N_2 = (1-\xi)(1+\eta)/4;\ N_3 = (1+\xi)(1+\eta)/4;$$
$$N_4 = (1+\xi)(1-\eta)/4;\ N_5 = (1-\xi^2)(1-\eta)/4;\ N_6 = (1-\xi)(1-\eta^2)/2;$$
$$N_7 = (1-\xi^2)(1+\eta)/2;\ N_8 = (1+\xi)(1-\eta^2)/2;\ N_9 = (1-\xi^2)(1-\eta^2) \tag{20}$$

In this part, the element nodal load vector and element stiffness matrix are derived for the static analysis. The equation of equilibrium and the element stiffness matrix listed below may be created with the use of the Hamilton principle.

Table 1 Validation of normalized fundamental frequency ($\bar{}$) for the simply supported square laminate of orientation angle 0°/90°/90°/0°

a/h	References	Theory	Frequency ($\bar{w}$)			
			E_1/E_2=10	E_1/E_2=20	E_1/E_2=30	E_1/E_2=40
5	Present study (12×12)	ITSDT	8.338	9.560	10.255	10.720
	Xiang and Wang (2009)	HSDT	8.421	9.671	10.416	10.938
	Liew et al. (2003)	HSDT	8.299	9.568	10.327	10.855
100	Present study (12×12)	ITSDT	9.854	12.235	13.875	15.100
	Xiang and Wang (2009)	HSDT	9.912	12.316	13.943	15.213

Table 2 New result of normalized fundamental frequency ($\bar{}$) for the simply supported square laminate of orientation angle 0°/90°/90°/0° having porosities ($p=0$)

a/h	References	Theory	Orientation angle	Frequency ($\overline{w}$)			
				E_1/E_2=10	E_1/E_2=20	E_1/E_2=30	E_1/E_2=40
10	Present	ITSDT	0°/90°/90°0°	9.854	12.242	13.877	15.100
			0°/60°/60°0°	9.931	12.382	14.005	15.253
			0°/45°/45°0°	9.974	12.415	14.081	15.319
			0°/30°/30°0°	9.975	12.418	14.076	15.314
20	Present	ITSDT	0°/90°/90°0°	10.402	13.428	15.744	17.644
			0°/60°/60°0°	10.481	13.548	15.892	17.814
			0°/45°/45°0°	10.522	13.609	15.968	17.902
			0°/30°/30°0°	10.516	13.591	15.945	17.877
50	Present	ITSDT	0°/90°/90°0°	10.579	13.838	16.438	18.657
			0°/60°/60°0°	10.659	13.961	16.592	18.836
			0°/45°/45°0°	10.699	14.019	16.665	18.920
			0°/30°/30°0°	10.689	13.996	16.632	18.881
100	Present	ITSDT	0°/90°/90°0°	10.611	13.907	16.552	18.824
			0°/60°/60°0°	10.692	14.031	16.707	19.004
			0°/45°/45°0°	10.731	14.088	16.779	19.087
			0°/30°/30°0°	10.721	14.063	16.744	19.045

Table 3 New result of normalized fundamental frequency ($\bar{}$) for the simply supported square laminate of orientation angle 0°/90°/90°/0° having porosities ($p=0.1$)

a/h	References	Theory	Orientation angle	Frequency ($\overline{w}$)			
				E_1/E_2=10	E_1/E_2=20	E_1/E_2=30	E_1/E_2=40
10	Present	ITSDT	0°/90°/90°0°	9.486	11.796	13.402	14.615
			0°/60°/60°0°	9.558	11.901	13.525	14.747
			0°/45°/45°0°	9.599	11.961	13.597	14.827
			0°/30°/30°0°	9.601	11.958	13.593	14.823
20	Present	ITSDT	0°/90°/90°0°	9.974	12.847	15.062	16.889
			0°/60°/60°0°	10.048	12.960	15.202	17.050
			0°/45°/45°0°	10.086	13.017	15.273	17.133
			0°/30°/30°0°	10.082	13.001	15.252	17.109
50	Present	ITSDT	0°/90°/90°0°	10.131	13.205	15.666	17.771
			0°/60°/60°0°	10.205	13.321	15.811	17.939
			0°/45°/45°0°	10.242	13.376	15.880	18.018
			0°/30°/30°0°	10.235	13.355	15.849	17.982
100	Present	ITSDT	0°/90°/90°0°	10.159	13.266	15.766	17.915
			0°/60°/60°0°	10.234	13.382	15.912	18.085
			0°/45°/45°0°	10.271	13.436	15.979	18.164
			0°/30°/30°0°	10.264	13.414	15.947	18.125

$$\left[k^{el}\right] = \sum_{i=1}^{nu+nl} \iiint [B]^T[H]^T\left[Q^{-i}\right][H][B]dxdydz + \left[p_0\right] \quad (21)$$

$$\left[k^{el}\right] = \sum_{i=1}^{nu+nl} \iint [B]^T[D][B]dxdy + \left[p_0\right] \quad (22)$$

where $[B]$ is the strain matrix, $[Q]$ is the converted material constant matrix and $[H]$ is the matrix consists of terms containing z and material properties term.

where $[D] = \int_{k=1}^{n} \int [H]^T\left[Q^{-i}\right][H]dz$.

Now, using Eq. 15, the sanction term is represented as

$$\left[p_0\right] = \iint \mu\left(\left\{\frac{\delta w}{\delta x} - w_1\right\}\left\{\frac{\delta w}{\delta x} - w_1\right\} + \left\{\frac{\delta w}{\delta y} - w_2\right\}\left\{\frac{\delta w}{\delta y} - w_2\right\}\right)dxdy \quad (23)$$

where μ is the sanction parameter.

With the use of Eq. 19, the element load vector may also be obtained throughout the computation process and shown as

$$\left[p_0\right] = \int [N]^T q dxdy \quad (24)$$

Table 4 New result of normalized fundamental frequency ($\bar{}$) for the simply supported square laminate of orientation angle 0°/90°/90°/0° having porosities ($p=0.2$)

a/h	References	Theory	Orientation angle	Frequency ($\overline{w}$)			
				E_1/E_2=10	E_1/E_2=20	E_1/E_2=30	E_1/E_2=40
10	Present	ITSDT	0°/90°/90°0°	9.096	11.313	12.880	14.077
			0°/60°/60°0°	9.162	11.412	12.997	14.205
			0°/45°/45°0°	9.200	11.468	13.066	14.283
			0°/30°/30°0°	9.203	11.466	13.062	14.278
20	Present	ITSDT	0°/90°/90°0°	9.524	12.231	14.333	16.078
			0°/60°/60°0°	9.592	12.336	14.465	16.230
			0°/45°/45°0°	9.628	13.390	14.532	16.308
			0°/30°/30°0°	9.625	13.376	14.512	16.285
50	Present	ITSDT	0°/90°/90°0°	9.661	12.539	14.851	16.833
			0°/60°/60°0°	9.729	12.645	14.987	16.991
			0°/45°/45°0°	9.764	12.698	15.051	17.066
			0°/30°/30°0°	9.759	12.679	15.024	17.032
100	Present	ITSDT	0°/90°/90°0°	9.687	12.592	14.937	16.956
			0°/60°/60°0°	9.755	12.699	15.073	17.116
			0°/45°/45°0°	9.789	12.750	15.137	17.190
			0°/30°/30°0°	9.785	12.731	15.108	17.154

where q is the magnitude of the transverse load and is $[N]$ the matrix representing the shape function, respectively.

Element mass matrix

For free vibration problem, the acceleration at any point within the plate is can be expressed in form of reference plane parameters with the help of Eqs. (4)–(6) as

$$\left\{\ddot{f}\right\} = -\omega^2 \begin{Bmatrix} \overline{u}_1 \\ \overline{u}_2 \\ \overline{w} \end{Bmatrix} \tag{25}$$

$$\left\{\ddot{f}\right\} = -\omega^2 [F]\{f\} \tag{26}$$

where the matrix $[F]$ is the order of 3×7 contains z and some constant qualities like that of $[H]$ and

Table 5 New result of normalized fundamental frequency ($\bar{}$) for the simply supported square laminate of orientation angle 0°/90°/90°/0° having porosities ($p=0.3$)

a/h	References	Theory	Orientation angle	Frequency ($\overline{w}$)			
				E_1/E_2=10	E_1/E_2=20	E_1/E_2=30	E_1/E_2=40
10	Present	ITSDT	0°/90°/90°0°	8.678	10.786	12.303	13.477
			0°/60°/60°0°	8.738	10.879	12.414	13.599
			0°/45°/45°0°	8.773	10.931	12.448	13.672
			0°/30°/30°0°	8.778	10.929	12.475	13.668
20	Present	ITSDT	0°/90°/90°0°	9.049	11.572	13.552	15.203
			0°/60°/60°0°	9.110	11.670	13.673	15.344
			0°/45°/45°0°	9.143	11.720	13.736	15.417
			0°/30°/30°0°	9.143	11.708	13.718	15.396
50	Present	ITSDT	0°/90°/90°0°	9.167	11.834	13.986	15.836
			0°/60°/60°0°	9.228	11.932	14.112	15.983
			0°/45°/45°0°	9.260	12.480	14.171	16.052
			0°/30°/30°0°	9.259	11.965	14.147	16.022
100	Present	ITSDT	0°/90°/90°0°	9.189	11.879	14.058	15.939
			0°/60°/60°0°	9.251	11.978	14.184	16.087
			0°/45°/45°0°	9.283	12.025	14.245	16.156
			0°/30°/30°0°	9.281	12.009	14.218	16.124

Table 6 Validation of normalized fundamental frequency ($\bar{}$) for the simply supported square laminate of orientation angle 0°/90°/0° with different boundary condition

Boundary condition	References	Theory	a/h			
			10	20	50	100
SSSS	Present study	ITSDT	11.667	13.955	14.936	15.101
	Khdeir and Reddy (1999)	SSDT	12.527	14.377	15.081	15.191
	Librescu et al. (1989)	HSDT	11.958			
		FSTDT	12.163			
		CPT	15.104			
SSSC	Present study	ITSDT	13.748	18.749	21.897	22.520
	Khdeir and Reddy (1999)	SSDT	14.981	19.681	22.164	22.604
	Librescu et al. (1989)	TSDT	13.815			
		FSDT	14.248			
		CPT	22.557			
SSCC	Present study	ITSDT	16.003	23.923	30.431	31.923
	Khdeir and Reddy (1999)	SSDT	17.458	25.434	30.886	31.991
	Librescu et al. (1989)	TSDT	15.739			
		FSDT	16.383			
		CPT	32.093			
SSFS	Present study	ITSDT	4.288	4.379	4.412	4.420
	Khdeir and Reddy (1999)	SSDT	4.343	4.457	4.493	4.499
	Librescu et al. (1989)	TSDT	4.323			
		FSDT	4.320			
		CPT	4.485			
SSFC	Present study	ITSDT	6.054	6.573	6.769	6.802
	Khdeir and Reddy (1999)	SSDT	6.241	6.695	6.853	6.878
	Librescu et al. (1989)	TSDT	6.095			
		FSDT	6.144			
		CPT	6.863			

Table 7 New result of normalized fundamental frequency ($\bar{}$) for the simply supported square laminate of different boundary conditions having porosities ($p=0$)

Boundary condition	References	Theory	Orientation angle	a/h			
				10	20	50	100
SSSS	Present	ITSDT	0°/90°/0°	11.667	13.955	14.936	15.101
			0°/60°/0°	12.054	14.179	15.066	15.214
			0°45°/0°	12.364	14.359	15.160	15.294
			0°/30°/0°	12.622	14.478	15.191	15.309
SSSC	Present	ITSDT	0°/90°/0°	13.748	18.749	21.897	22.520
			0°/60°/0°	14.263	19.178	22.091	22.654
			0°45°/0°	14.795	19.608	22.279	22.783
			0°/30°/0°	15.369	20.028	22.439	22.884
SSCC	Present	ITSDT	0°/90°/0°	16.003	23.923	30.431	31.923
			0°/60°/0°	16.605	24.598	30.718	32.091
			0°45°/0°	17.329	25.353	31.057	32.290
			0°/30°/0°	18.197	26.175	31.409	32.502
SSFS	Present	ITSDT	0°/90°/0°	4.288	4.379	4.412	4.420
			0°/60°/0°	4.006	4.102	4.139	4.148
			0°45°/0°	3.816	3.913	3.951	3.960
			0°/30°/0°	3.672	3.767	3.804	3.812
SSFC	Present	ITSDT	0°/90°/0°	6.054	6.573	6.769	6.802
			0°/60°/0°	5.903	6.421	6.615	6.649
			0°45°/0°	5.844	6.350	6.536	6.569
			0°/30°/0°	5.844	6.316	6.486	6.516

Table 8 New result of normalized fundamental frequency ($\bar{}$) for the simply supported square laminate of different boundary conditions having porosities ($p=0.1$)

Boundary condition	References	Theory	Orientation angle	a/h			
				10	20	50	100
SSSS	Present	ITSDT	0°/90°/0°	11.318	13.379	14.237	14.379
			0°/60°/0°	11.676	13.584	14.357	14.486
			0°45°/0°	11.963	13.748	14.447	14.563
			0°/30°/0°	12.201	13.855	14.477	14.579
SSSC	Present	ITSDT	0°/90°/0°	13.454	18.097	20.881	21.423
			0°/60°/0°	13.949	18.490	21.060	21.549
			0°45°/0°	14.460	18.882	21.233	21.671
			0°/30°/0°	15.007	19.263	21.379	21.766
SSCC	Present	ITSDT	0°/90°/0°	15.749	23.233	29.053	30.368
			0°/60°/0°	16.337	23.859	29.328	30.523
			0°45°/0°	17.047	24.557	29.634	30.708
			0°/30°/0°	17.890	25.312	29.953	30.906
SSFS	Present	ITSDT	0°/90°/0°	4.121	4.203	4.234	4.241
			0°/60°/0°	3.859	3.947	3.981	3.990
			0°45°/0°	3.683	3.772	3.807	3.816
			0°/30°/0°	3.549	3.637	3.672	3.681
SSFC	Present	ITSDT	0°/90°/0°	5.827	6.297	6.472	6.503
			0°/60°/0°	5.687	6.156	6.330	6.361
			0°45°/0°	5.634	6.090	6.257	6.286
			0°/30°/0°	5.633	6.059	6.211	6.238

Table 9 New result of normalized fundamental frequency ($\bar{}$) for the simply supported square laminate of different boundary conditions having porosities ($p=0.2$)

Boundary condition	References	Theory	Orientation angle	a/h			
				10	20	50	100
SSSS	Present	ITSDT	0°/90°/0°	10.930	12.759	13.496	13.618
			0°/60°/0°	11.258	12.945	13.609	13.719
			0°45°/0°	11.521	13.093	13.693	13.792
			0°/30°/0°	11.737	13.189	13.722	13.810
SSSC	Present	ITSDT	0°/90°/0°	13.121	17.377	19.801	20.262
			0°/60°/0°	13.593	17.732	19.962	20.380
			0°45°/0°	14.078	18.086	20.120	20.494
			0°/30°/0°	14.595	18.427	20.253	20.585
SSCC	Present	ITSDT	0°/90°/0°	15.448	22.454	27.590	28.716
			0°/60°/0°	16.030	23.028	27.836	28.859
			0°45°/0°	16.721	23.665	28.110	29.031
			0°/30°/0°	17.532	24.349	28.396	29.215
SSFS	Present	ITSDT	0°/90°/0°	3.944	4.020	4.048	4.055
			0°/60°/0°	3.704	3.785	3.817	3.825
			0°45°/0°	3.542	3.625	3.658	3.666
			0°/30°/0°	3.421	3.503	3.535	3.543
SSFC	Present	ITSDT	0°/90°/0°	5.584	6.005	6.161	6.188
			0°/60°/0°	5.457	5.876	6.030	6.057
			0°45°/0°	5.408	5.816	5.964	5.590
			0°/30°/0°	5.408	5.788	5.923	5.948

Table 10 New result of normalized fundamental frequency ($\bar{}$) for the simply supported square laminate of different boundary conditions having porosities ($p=0.3$)

Boundary condition	References	Theory	Orientation angle	a/h			
				10	20	50	100
SSSS	Present	ITSDT	0°/90°/0°	10.496	12.088	12.709	12.811
			0°/60°/0°	10.791	12.254	12.813	12.905
			0°45°/0°	11.027	12.386	12.891	12.975
			0°/30°/0°	11.221	12.471	12.920	12.994
SSSC	Present	ITSDT	0°/90°/0°	12.740	16.576	18.640	19.026
			0°/60°/0°	13.184	16.891	18.785	19.135
			0°45°/0°	13.639	17.205	18.928	19.242
			0°/30°/0°	14.119	17.506	19.048	19.327
SSCC	Present	ITSDT	0°/90°/0°	15.106	21.567	26.007	26.952
			0°/60°/0°	15.671	22.084	26.223	27.083
			0°45°/0°	16.335	22.655	26.466	27.241
			0°/30°/0°	17.107	23.265	26.720	27.410
SSFS	Present	ITSDT	0°/90°/0°	3.757	3.827	3.853	3.859
			0°/60°/0°	3.541	3.615	3.645	3.652
			0°45°/0°	3.395	3.472	3.503	3.510
			0°/30°/0°	3.287	3.362	3.393	3.400
SSFC	Present	ITSDT	0°/90°/0°	5.322	5.696	5.832	5.856
			0°/60°/0°	5.208	5.579	5.714	5.738
			0°45°/0°	5.165	5.525	5.655	5.678
			0°/30°/0°	5.165	5.500	5.620	5.642

$$\{f\} = \begin{bmatrix} u_1 & u_2 & u_3 & \psi_1 & \psi_2 & w_1 & w_2 \end{bmatrix}^T \tag{27}$$

Finally, it may be expressed in terms of nodal displacement vector $\{\delta\}$ with the help of Eq. 19 as

$$\{f\} = [C]\{\delta\} \tag{28}$$

where the matrix $[C]$ is an order of 7×63 and $[N_1]$, $[N_2]$ along with its derivatives.

Now using the above Eqs. (25)–(28), the consistent mass matrix of an element can be derived as

$$[m^e] = \sum_{i=1}^{nu+nl} \int \rho_i [C]^T [F]^T [F][C] dxdydz = \int [C]^T [L][C] dxdy \tag{29}$$

where ρ_i is the mass density of the ith layer and $[C]$ is the shape function matrix and the matrix $[L]$ is expressed as

$$[L] = \int \rho_i [F]^T [F] dz \tag{30}$$

Free vibration analysis

In the governing Eq. (1) is solved by the simultaneous iteration technique for the calculation of eigen values and eigen vectors. In this method $[K]$ is positive definite and can be expressed as

$$[K] = [L][T]^T \tag{31}$$

$$\left\{[L]^{-1}[M][L]^{-T}\right\}[L]^T\{\delta\} = \frac{1}{\omega^2}[L]^T\{\delta\} \tag{32}$$

In the above equation, it is solved for the exact eigen value and eigen vectors. In this Eq. $1/\omega^2$ is the eigen value. Therefore, the eigen value crossholdings to the natural frequency. The non-dimensional natural frequencies are computed as

$$\overline{\omega} = \frac{\omega a^2}{h}\sqrt{\frac{\rho}{E_2}} \tag{33}$$

Results and discussion

In the present research article, many examples are discussed for the vibration analysis of the laminated porous plate using a finite element model. A convergence study is carried out to determine the accuracy and applicability of the finite element model. In the present analysis, improved third-order shear deformation is carried out throughout the entire discussion. I selected a 12×12 mesh size of the plate in the entire discussion. In addition to it, a different porosity distribution is introduced in relation to the thickness of the plate, like 0.1, 0.2, and 0.3. In the result and discussion portions, a change in the angle of orientation of the fibre is also experienced as an effect of the vibration analysis.

Table 11 Validation of normalized fundamental frequency ($\bar{}$) for the simply supported square laminate of orientation angle 0°/90° with different boundary condition

Boundary condition	References	Theory	a/h			
			05	10	20	50
SSSS	Present study	ITSDT	7.644	8.732	9.130	9.262
	Khdeir and Reddy (1999)	SSDT	7.609	8.997	9.504	9.665
	Librescu et al. (1989)	HSDT		8.944		
		FSDT		8.900		
		CPT		9.566		
SSSC	Present study	ITSDT	8.897	10.793	11.619	11.914
	Khdeir and Reddy (1999)	SSDT	8.454	10.803	11.872	12.247
	Librescu et al. (1989)	HSDT		10.662		
		FSDT		10.612		
		CPT		12.145		
SSCC	Present study	ITSDT	10.331	13.378	15.003	15.649
	Khdeir and Reddy (1999)	SSDT	9.377	12.959	15.015	15.835
	Librescu et al. (1989)	HSDT		12.673		
		FSDT		12.622		
		CPT		15.771		
SSFF	Present study	ITSDT	5.230	5.717	6.086	6.166
	Khdeir and Reddy (1999)	SSDT	5.046	5.818	6.080	6.216
	Librescu et al. (1989)	HSDT		5.796		
		FSDT		5.774		
		CPT		6.136		
SSFS	Present study	ITSDT	5.206	5.962	6.215	6.296
	Khdeir and Reddy (1999)	SSDT	5.315	6.150	6.440	7.212
	Librescu et al. (1989)	HSDT		6.123		
		FSDT		6.100		
		CPT		6.500		
SSFC	Present study	ITSDT	5.553	6.451	6.720	6.807
	Khdeir and Reddy (1999)	SSDT	5.675	6.603	6.936	8.365
	Librescu et al. (1989)	HSDT		6.566		
		FSDT		6.544		
		CPT		7.014		

Example 1 This problem is solved to access the performance of the proposed finite element model for the free vibration analysis of laminated plates. The validation study of the present research is shown in Table 1, and new results have been obtained for the different porosity distributions, angles of orientation, and material properties, etc. A four-layered simply supported square ($a=b$) plate has an angle of orientation of 0°/90°/90°/0° and the material properties of each individual layer are considered as: E_1/E_2=open, $G_{12}=G_{13}=0.6E_2$, $G_{23}=0.5E_2$, $\upsilon_{12}=\upsilon_{13}=0.25$ and $\rho = 1$. The non-dimensional natural frequencies are obtained as

$$\overline{\omega} = \frac{\omega a^2}{h}\sqrt{\frac{\rho}{E_2}}.$$

The normalised fundamental frequency parameter obtained by the present finite element model with various modulus ratios, thickness ratios, and changes in orientation angles of the laminated porous composite plate. A detailed discussion is carried out for the normalised fundamental frequency in Tables 2, 3, and 4 having different porosity distributions along the thickness of the plate with the help of improved third-order deformation theory. In Table 2, by decreasing the orientation angle of the laminated fiber, the normalised fundamental frequency increases for any modulus ratio like 10, 20, 30, or 40. In Table 2, all results have been shown without porosity distribution, like ($p=0$). For a thickness ratio and modulus ratio of 10, the frequency is increased by 1.2% for the change in angle of orientation from 0°/90°/90°0° to 0°/30°/30°0° and is also increases by approximately 1.4% for modulus ratio 20, 30, and 40. In Table 2, there seems to be no major change in normalised frequency by changing the angle of orientation of the laminate. But by changing the modulus ratio from 10 to 20 for a particular orientation angle, there is a major change in frequency of about 24.23%. Now in Table 3, a porosity of 0.1 is introduced in the entire thickness of the plate, and the frequency is reduced by 3.7% for the thickness and modulus ratio of 10 and orientation angle of 0°/90°/90°/0°. In Table 3, for a modulus ratio of 30 and an orientation angle of 0°/90°/90°0°, the frequency increases by 16.84% due to a change in a thickness ratio of 10 to 20. In Table 4, the frequency is

Table 12 New result of normalized fundamental frequency ($\bar{}$) for the simply supported square laminate of different boundary conditions having porosities ($p=0$)

Boundary condition	References	Theory	Orientation angle	a/h			
				05	10	20	50
SSSS	Present	ITSDT	0°/90°	7.644	8.732	9.130	9.260
			0°/60°	7.915	9.150	9.622	9.778
			0°/45°	8.308	9.945	10.604	10.827
			0°/30°	8.905	11.266	12.289	12.646
SSSC	Present	ITSDT	0°/90°	8.897	10.793	11.619	11.914
			0°/60°	9.071	11.237	12.241	12.608
			0°/45°	9.243	11.973	13.353	13.879
			0°/30°	9.553	13.225	15.322	16.173
SSCC	Present	ITSDT	0°/90°	10.331	13.378	15.003	15.649
			0°/60°	10.371	13.828	15.771	16.561
			0°/45°	10.308	14.542	17.146	18.256
			0°/30°	10.430	15.845	19.632	21.386
SSFF	Present	ITSDT	0°/90°	5.230	5.717	6.086	6.166
			0°/60°	5.384	5.809	6.213	6.309
			0°/45°	5.778	6.097	6.785	6.946
			0°/30°	6.593	6.641	8.122	8.455
SSFS	Present	ITSDT	0°/90°	5.206	5.962	6.215	6.296
			0°/60°	4.348	4.907	5.120	5.211
			0°/45°	3.704	4.113	4.268	4.336
			0°/30°	3.481	3.856	3.992	4.048
SSFC	Present	ITSDT	0°/90°	5.553	6.451	6.720	6.807
			0°/60°	4.757	5.375	5.621	5.727
			0°/45°	4.253	4.838	5.075	5.173
			0°/30°	4.339	5.121	5.444	5.568

decreased by 8.87% compared to Table 2 for the thickness ratio, modulus ratio, and orientation angle of 20, 40 and 0°/90°/90°/0°, respectively. In Table 4, the fundamental frequency is increased by 11%when then the thickness ratio is increased from 10 to 20 for the modulus ratio of 30 and orientation angle of 0°/30°/30°/0°. Now a porosity distribution of 0.3 is introduced in the entire thickness of the plate and seems to be normalized frequency is decreased by 13.88% compared to the porosity of $p=0$, for the thickness and modulus ratio of 20 having orientation angle of 0°/45°/45°/0°. In Table 5, the fundamental frequency is increased to 13.67% by a change in a thickness ratio of 10–50 due to a modulus ratio of 30 and orientation angle of 0°/60°/60°/0°.

Example 2 Fundamental frequencies for symmetric cross-ply laminated plates are presented in Tables 6, 7, 8, 9, and 10. In Table 6, a validation study is carried out for the accuracy and applicability of the finite element model with different boundary conditions. A three-layered symmetric cross-ply laminated simply supported square plate has an angle of orientation of 0°/90°/0° and the material properties of each individual layer are considered as: E_1/E_2=25, G_{12}=G_{13} =0.5E_2, G_{23}=0.2E_2, $\upsilon_{12}=\upsilon_{13}=0.25$ and $\rho=1$. The non-dimensional natural frequencies are obtained as

$$\overline{\omega}=\frac{\omega a^2}{h}\sqrt{\frac{\rho}{E_2}}.$$

All layers are assumed to be the same thickness, density, and made of the same orthotropic material. The boundary condition and coordinates of the laminate are as follows: the edges $x_1=0,a$ are assumed as simply supported while $x_2=\pm b/2$ can take any combination of clamped (C), Free (F), and simply supported (S) edge conditions.

In Table 6, the result is validated with a different boundary condition for an orientation angle of 0°/90°/0° and new results are obtained in Tables 7, 8, 9, and 10 for laminated plates with different porosity, thickness ratio, orientation angle, and boundary conditions.

In Table 7, the normalised fundamental frequency is increased by decreasing the angle of orientation for different thickness ratios and boundary conditions. For the thickness ratio of 10, the fundamental frequency is increased by 8.2% by changing the orientation angle from 0°/90°/0° to 0°

Table 13 New result of normalized fundamental frequency ($\bar{}$) for the simply supported square laminate of different boundary conditions having porosities ($p=0.1$)

Boundary condition	References	Theory	Orientation angle	a/h			
				05	10	20	50
SSSS	Present	ITSDT	0°/90°	7.372	8.360	8.716	8.833
			0°/60°	7.654	8.792	9.218	9.359
			0°/45°	8.068	9.585	10.182	10.384
			0°/30°	8.688	10.874	11.797	12.115
SSSC	Present	ITSDT	0°/90°	8.625	10.355	11.089	11.349
			0°/60°	8.810	10.819	11.726	12.054
			0°/45°	9.016	11.576	12.834	13.308
			0°/30°	9.372	12.846	14.769	15.537
SSCC	Present	ITSDT	0°/90°	10.065	12.879	14.326	14.894
			0°/60°	10.122	13.361	15.119	15.824
			0°/45°	10.109	14.120	16.504	17.502
			0°/30°	10.294	15.480	18.989	20.578
SSFF	Present	ITSDT	0°/90°	5.031	5.463	5.781	5.851
			0°/60°	5.211	5.567	5.946	6.034
			0°/45°	5.625	5.880	6.535	6.685
			0°/30°	6.453	6.646	7.865	8.172
SSFS	Present	ITSDT	0°/90°	5.012	5.692	5.916	5.988
			0°/60°	4.209	4.719	4.909	4.991
			0°/45°	3.599	3.977	4.119	4.182
			0°/30°	3.383	3.730	3.856	3.907
SSFC	Present	ITSDT	0°/90°	5.471	6.167	6.406	6.485
			0°/60°	4.606	5.174	5.397	5.493
			0°/45°	4.131	4.673	4.889	4.979
			0°/30°	4.217	4.941	5.234	5.346

/30°/0° having edge condition SSSS. For boundary conditions of SSSC, frequency is decreased by 6.8% by changing the orientation angle from 0°/90°/0° to 0°/30°/0° having a thickness ratio of 20. As shown in Table 8, the fundamental frequency is reduced by 3.14% due to the porosity effect ($p=0$ to $p=0.1$) having SSCC boundary conditions. Now for the thickness ratio of 50 frequency is reduced by10% due to a change in orientation angle from 0°/90°/0° to 0°/45°/0° and having edge condition of the plate is SSFS. In Table 9, fundamental frequency is increased by 8.4% by changing the orientation angle from 0°/90°/0° to 0°/30°/0° for the SSCC end condition and having a thickness ratio of 20. Normalized fundamental frequency increases with decreasing orientation angle for a given thickness ratio. Now in Table 10, when the thickness ratio increases, the fundamental frequency also increases for any particular edge condition and orientation angle of the laminate. By introducing a porosity of 0.3, the frequency further decreases as compared to Table 7. For the SSFS edge condition, the frequency decreases by 9% by a change in orientation angle from 0°/90°/0° to 0°/45°/0° with a thickness ratio of 100.

Example 3 Two layered antisymmetric cross-ply laminated square plate having an orientation angle of 0°/90° is analysed for different boundary condition. Material properties are as follows: $E_1/E_2=25$, $G_{12}=G_{13}=0.5E_2$, $G_{23}=0.2E_2$, $\upsilon_{12}=\upsilon_{13}=0.25$ and $\rho=1$. Normal fundamental frequency is calculated the same as the previous example. In Table 11 result is validated and a new result has been obtained in Tables 12, 13, 14, and 15.

In Table 12 different angle of orientation has been applied in the anti-symmetric laminated plate with different boundary conditions. It seems to be normalized that fundamental frequency increases as decreases thickness of the plate. In most cases, boundary condition frequency is increased by a decrease in orientation angle of the laminate. Now for the edge condition, SSFC frequency decreases by 16.34% by decreasing the orientation angle from 0°/90° to 0°/60°. A porosity distribution is $p=0.1$ is induced in the entire thickness of the plate and the result is shown in Table 13 for the thickness ratio of 100 and orientation angle of 0° /60° fundamental frequency is decreased by 3.6% with edge condition SSSS. For a thickness ratio of 5 fundamental frequency is decreased by 19.8% having edge condition SSFC of the laminated plate.it seems to be frequency is decreased by 11.79% with a change in orientation angle of the anti-symmetric plate from 0°/90° to 0°/45° having thickness ratio

Table 14 New result of normalized fundamental frequency ($\bar{}$) for the simply supported square laminate of different boundary conditions having porosities ($p = 0.2$)

Boundary condition	References	Theory	Orientation angle	a/h			
				05	10	20	50
SSSS	Present	ITSDT	0°/90°	7.075	7.965	8.280	8.383
			0°/60°	7.371	8.411	8.793	8.919
			0°/45°	7.807	9.200	9.737	9.918
			0°/30°	8.447	10.450	11.273	11.554
SSSC	Present	ITSDT	0°/90°	8.323	9.884	10.527	10.754
			0°/60°	8.524	10.371	11.181	11.471
			0°/45°	8.767	11.148	12.284	12.706
			0°/30°	9.170	12.429	14.178	14.864
SSCC	Present	ITSDT	0°/90°	9.767	12.334	13.603	14.095
			0°/60°	9.846	12.852	14.425	15.046
			0°/45°	9.888	13.659	15.819	16.708
			0°/30°	10.142	15.078	18.297	19.722
SSFF	Present	ITSDT	0°/90°	4.810	5.190	5.456	5.518
			0°/60°	5.022	5.310	5.664	5.744
			0°/45°	5.457	5.648	6.272	6.409
			0°/30°	6.297	6.237	7.591	7.870
SSFS	Present	ITSDT	0°/90°	4.801	5.404	5.599	5.662
			0°/60°	4.057	4.516	4.685	4.757
			0°/45°	3.484	3.832	3.961	4.018
			0°/30°	3.276	3.596	3.653	3.758
SSFC	Present	ITSDT	0°/90°	5.242	5.865	6.075	6.144
			0°/60°	4.441	4.959	5.159	5.245
			0°/45°	3.998	4.497	4.694	4.776
			0°/30°	4.085	4.748	5.011	5.112

10 and boundary condition is SSSC. Now a porosity of 0.2 is introduced in the entire thickness of the plate and results have been shown in Table 14. For the edge condition, SSSS frequency is increased by 6.37% when the orientation angle changes from 0°/90° to 0°/60° with a thickness ratio of 5. In Table 14 fundamental frequency is increased by approximately 9% with a change in orientation angle 0°/90° to 0° /45° having a thickness ratio of 10.

For the free vibration analysis of the laminated porous plate, a porosity of 0.3 is introduced in the entire thickness of the plate and the fundamental frequency is obtained as shown in Table 15. Further decrease in fundamental frequency as compared to Tables 13 and 14 in some edge conditions such as SSSS, SSSC, SSCC and SSFF. In boundary conditions, SSFS and SSFC fundamental frequencies are decreased for the entire thickness ratio like 5, 10, 20, and 50. For the thickness ratio of 50 normalized fundamental frequency is decreased by 12.72% with a change in orientation angle from 0°/90° to 0°/60° having edge condition SSFS. Normalized fundamental frequency is also decreased by approximately 6%, while a change in orientation angle from 0°/45° to 0°/30° having a thickness ratio of 10.

Conclusion

Free vibration analysis of laminated composite porous plate analysed with improved third-order theory. It analysed different boundary conditions and porosity distributions. The main outcomes of the present research article are listed below.

- The fundamental frequency decreases with porosity distribution in the entire thickness of the plate, like $p = 0.0$, 0.1, 0.2, 0.3.
- The fibre orientation angle is a significant change in the normal frequency of the laminated plate.
- In most of the boundary conditions like SSSS, SSSC, SSCC, and SSFF, the fundamental frequency increases with the decrease in orientation angle, like from 0°/90° /0 to 0°/30°/0°.
- In SSFS and SSFC edge conditions, fundamental frequency is increased with a change in orientation angle from 0°/90°/0 to 0°/30°/0°.
- For the modulus ratio of 40 and the thickness ratio of 10, the normalised fundamental frequency is increased

Table 15 New result of normalized fundamental frequency ($\bar{}$) for the simply supported square laminate of different boundary conditions having porosities ($p = 0.3$)

Boundary condition	References	Theory	Orientation angle	a/h			
				05	10	20	50
SSSS	Present	ITSDT	0°/90°	6.749	7.541	7.817	7.906
			0°/60°	7.064	8.004	8.342	8.454
			0°/45°	7.522	8.787	9.265	9.424
			0°/30°	8.176	9.989	10.712	10.957
SSSC	Present	ITSDT	0°/90°	7.984	9.372	9.927	10.122
			0°/60°	8.207	9.886	10.599	10.854
			0°/45°	8.492	10.684	11.696	12.069
			0°/30°	8.943	11.973	13.542	14.146
SSCC	Present	ITSDT	0°/90°	9.428	11.732	12.825	13.245
			0°/60°	9.536	12.294	13.680	14.221
			0°/45°	9.640	13.152	15.085	15.866
			0°/30°	9.968	14.627	17.545	18.806
SSFF	Present	ITSDT	0°/90°	4.709	4.880	5.110	5.163
			0°/60°	4.892	5.034	5.363	5.436
			0°/45°	5.271	5.401	5.991	6.117
			0°/30°	6.149	6.013	7.295	7.545
SSFS	Present	ITSDT	0°/90°	4.566	5.094	5.262	5.316
			0°/60°	3.887	4.295	4.443	4.506
			0°/45°	3.357	3.676	3.789	3.841
			0°/30°	3.159	3.451	3.555	3.598
SSFC	Present	ITSDT	0°/90°	4.991	5.540	5.723	5.783
			0°/60°	4.261	4.727	4.905	4.982
			0°/45°	3.853	4.309	4.486	4.560
			0°/30°	4.940	4.541	4.775	4.864

by 1.4% with a change in orientation angle 0°/90° /90° /0° to 0°/30°/30° /0°.

- With a porosity distribution of 0.1 in the entire thickness of the plate fundamental frequency is decreased by 3.2% for the modulus ratio of 40 and orientation angle 0°/90°/90° /0°.
- For the thickness ratio of 100 and modulus ratio of 10, the normalised fundamental frequency is decreased by 13.4% with a porosity of 0.3 and orientation angle of 0°/90°/90° /0°.
- For the boundary condition SSSC, fundamental frequency is decreased by 4.87% with a thickness ratio of 100 and orientation angle 0°/90°/0.
- With a change in orientation angle of 0°/90°/0 to 0°/30° /0°, the fundamental frequency is decreased by 14.36% for the boundary condition of SSFS.
- With a porosity distribution of 0.2 in the laminated plate, frequency is decreased by 7.76% with an edge condition of SSFC.
- For an antisymmetric laminated plate of 0°/90° and edge condition of SSSS, frequency is reduced by 3.6% due to a porosity value of 0.1.
- With boundary condition SSFF, the fundamental frequency is decreased by 8.0% due to a porosity distribution of 0.2 in the entire thickness of the laminated plate.
- As introduced porosity of 0.3 in a laminated simply supported square plate, the fundamental frequency decreases by 9.46% for the orientation angle of 0°/45°.

Author contributions The research was conducted by the first author, who also evaluated all the findings. The instructions, concepts, and formatting for the whole work were given by the second author.

Funding No particular grant from a financial organisation was given for this study.

Data availability No dataset used in the proposed work. The results are obtained based on numerical analysis.

Declarations

Competing interests The authors declare no competing interests.

Conflict of interest The authors state that they have no conflicts of interest.

References

Alambeigi, K., Mohammadimehr, M., Bamdad, M., & Rabczuk, T. (2020). Free and forced vibration analysis of a sandwich beam considering porous core and SMA hybrid composite face layers on Vlasov's foundation. *Acta Mechanica, 231*(8), 3199–3218. https://doi.org/10.1007/s00707-020-02697-5

Arshid, E., & Khorshidvand, A. R. (2018). Free vibration analysis of saturated porous FG circular plates integrated with piezoelectric actuators via differential quadrature method. *Thin-Walled Structures, 125*(November 2016), 220–233. https://doi.org/10.1016/j.tws.2018.01.007

Balak, M., Mehrabadi, S. J., Monfared, H. M., & Feizabadi, H. (2021). Free vibration analysis of a composite elliptical plate made of a porous core and two piezoelectric layers. *Proceedings of the Institution of Mechanical Engineers, Part l: Journal of Materials: Design and Applications, 235*(4), 796–812. https://doi.org/10.1177/1464420720973236

Belarbi, M. O., Tati, A., Ounis, H., & Khechai, A. (2017). On the free vibration analysis of laminated composite and sandwich plates: A layerwise finite element formulation. *Latin American Journal of Solids and Structures, 14*(12), 2265–2290. https://doi.org/10.1590/1679-78253222

Belarbi, M. O., Zenkour, A. M., Tati, A., Salami, S. J., Khechai, A., & Houari, M. S. A. (2021). An efficient eight-node quadrilateral element for free vibration analysis of multilayer sandwich plates. *International Journal for Numerical Methods in Engineering, 122*(9), 2360–2387. https://doi.org/10.1002/nme.6624

Benachour, A., Tahar, H. D., Atmane, H. A., Tounsi, A., & Ahmed, M. S. (2011). A four variable refined plate theory for free vibrations of functionally graded plates with arbitrary gradient. *Composites Part b: Engineering, 42*(6), 1386–1394. https://doi.org/10.1016/j.compositesb.2011.05.032

Bhardwaj, H. K., Vimal, J., & Sharma, A. K. (2015). Study of free vibration analysis of laminated composite plates with triangular cutouts. *Engineering Solid Mechanics, 3*(1), 43–50. https://doi.org/10.5267/j.esm.2014.11.002

Bîrsan, M., Altenbach, H., Sadowski, T., Eremeyev, V. A., & Pietras, D. (2012). Deformation analysis of functionally graded beams by the direct approach. *Composites Part b: Engineering, 43*(3), 1315–1328. https://doi.org/10.1016/j.compositesb.2011.09.003

Cheung, Y. K., & Zhou, D. (2001). Free vibrations of rectangular unsymmetrically laminated composite plates with internal line supports. *Computers and Structures, 79*(20–21), 1923–1932. https://doi.org/10.1016/S0045-7949(01)00096-7

Devarajan, B. (2021). *Free Vibration analysis of Curvilinearly Stiffened Composite plates with an arbitrarily shaped cutout using Isogeometric Analysis*. Preprint retrieved from http://arxiv.org/abs/2104.12856

Ebrahimi, F., Jafari, A., & Barati, M. R. (2017). Free vibration analysis of smart porous plates subjected to various physical fields considering neutral surface position. *Arabian Journal for Science and Engineering, 42*(5), 1865–1881. https://doi.org/10.1007/s13369-016-2348-3

Ferreira, A. J. M., & Fasshauer, G. E. (2006). Computation of natural frequencies of shear deformable beams and plates by an RBF-pseudospectral method. *Computer Methods in Applied Mechanics and Engineering, 196*(1–3), 134–146. https://doi.org/10.1016/j.cma.2006.02.009

Ferreira, A. J. M., Roque, C. M. C., Neves, A. M. A., Jorge, R. M. N., Soares, C. M. M., & Liew, K. M. (2011). Buckling and vibration analysis of isotropic and laminated plates by radial basis functions. *Composites Part b: Engineering, 42*(3), 592–606. https://doi.org/10.1016/j.compositesb.2010.08.001

Ghasemi, A. R., & Meskini, M. (2019). Free vibration analysis of porous laminated rotating circular cylindrical shells. *Jvc/journal of Vibration and Control, 25*(18), 2494–2508. https://doi.org/10.1177/1077546319858227

Gurjar, S. S., Narwariya, M., & Bansal, A. (2017). Vibration analysis of moderately thick symmetric cross laminated composite plate using FEM. *International Journal of Scientific Research in Science, Engineering and Technology*, *3*(3), 500–510.

Jianwei, S., Akihiro, N., & Hiroshi, K. (2004). Approximate vibration analysis of laminated curved panel using higher-order shear deformation theory. *Acta Mechanica Sinica*, *20*, 238–246.

Khdeir, A. A., & Reddy, J. N. (1999). Free vibrations of laminated composite plates using second-order shear deformation theory. *Computers and Structures, 71*(6), 617–626. https://doi.org/10.1016/S0045-7949(98)00301-0

Kim, G., Han, P., An, K., Choe, D., Ri, Y., & Ri, H. (2021a). Free vibration analysis of functionally graded double-beam system using Haar wavelet discretization method. *Engineering Science and Technology, an International Journal, 24*(2), 414–427. https://doi.org/10.1016/j.jestch.2020.07.009

Kim, K., Kwak, S., Jang, P., Sok, M., Jon, S., & Ri, K. (2021b). Free vibration analysis of elastically connected composite laminated double-plate system with arbitrary boundary conditions by using meshfree method. *AIP Advances, 11*(3), 035119, 1–17. https://doi.org/10.1063/5.0040270

Kumar, V., Singh, S. J., Saran, V. H., & Harsha, S. P. (2021). Vibration characteristics of porous FGM plate with variable thickness resting on Pasternak's foundation. *European Journal of Mechanics, A/Solids, 85*(July 2020), 104124. https://doi.org/10.1016/j.euromechsol.2020.104124

Li, Y. X., Hu, Z. J., & Sun, L. Z. (2016). Dynamical behavior of a double-beam system interconnected by a viscoelastic layer. *International Journal of Mechanical Sciences, 105*, 291–303. https://doi.org/10.1016/j.ijmecsci.2015.11.023

Li, Y. X., & Sun, L. Z. (2016). Transverse vibration of an undamped elastically connected double-beam system with arbitrary boundary conditions. *Journal of Engineering Mechanics, 142*(2), 1–18. https://doi.org/10.1061/(asce)em.1943-7889.0000980

Librescu, L., Khdeir, A. A., & Frederick, D. (1989). *I : Free u. 33*.

Liew, K. M. (2003). Vibration analysis of symmetrically laminated plates based on FSDT using the moving least squares differential quadrature method. *Computer Methods in Applied Mechanics and Engineering, 192*(19), 2203–2222. https://doi.org/10.1016/S0045-7825(03)00238-X

Liew, K. M., Huang, Y. Q., & Reddy, J. N. (2003). Vibration analysis of symmetrically laminated plates based on FSDT using the moving least squares differential quadrature method. *Computer Methods in Applied Mechanics and Engineering, 192*(19), 2203–2222. https://doi.org/10.1016/S0045-7825(03)00238-X

Liu, G. R., Zhao, X., Dai, K. Y., Zhong, Z. H., Li, G. Y., & Han, X. (2008). Static and free vibration analysis of laminated composite plates using the conforming radial point interpolation method. *Composites Science and Technology, 68*(2), 354–366. https://doi.org/10.1016/j.compscitech.2007.07.014

Magnucka-Blandzi, E., & Magnucki, K. (2007). Effective design of a sandwich beam with a metal foam core. *Thin-Walled Structures, 45*(4), 432–438. https://doi.org/10.1016/j.tws.2007.03.005

Merdaci, S. (2019). Free vibration analysis of composite material plates "Case of a typical functionally graded fg plates ceramic/metal" with porosities. *Nano Hybrids and Composites, 25*, 69–83. https://doi.org/10.4028/www.scientific.net/nhc.25.69

Muni Rami Reddy, R., Karunasena, W., & Lokuge, W. (2018). Free vibration of functionally graded-GPL reinforced composite plates with different boundary conditions. *Aerospace Science and Technology, 78*, 147–156. https://doi.org/10.1016/j.ast.2018.04.019

Nosier, A., Kapania, R. K., & Reddy, J. N. (1993). Free vibration analysis of laminated plates using a layerwise theory. *AIAA Journal, 31*(12), 2335–2346. https://doi.org/10.2514/3.11933

Palmeri, A., & Adhikari, S. (2011). A Galerkin-type state-space approach for transverse vibrations of slender double-beam systems with viscoelastic inner layer. *Journal of Sound and Vibration, 330*(26), 6372–6386. https://doi.org/10.1016/j.jsv.2011.07.037

Qatu, M. S. (1994). Natural frequencies for cantilevered laminated composite right triangular and trapezoidal plates. *Composites Science and Technology, 51*(3), 441–449. https://doi.org/10.1016/0266-3538(94)90112-0

Qu, Y., Long, X., Yuan, G., & Meng, G. (2013). A unified formulation for vibration analysis of functionally graded shells of revolution with arbitrary boundary conditions. *Composites, Part b: Engineering*. https://doi.org/10.1016/j.compositesb.2013.02.028

Rezaei, A. S., & Saidi, A. R. (2016). Application of Carrera Unified Formulation to study the effect of porosity on natural frequencies of thick porous-cellular plates. *Composites Part b: Engineering, 91*, 361–370. https://doi.org/10.1016/j.compositesb.2015.12.050

Rezaei, A. S., Saidi, A. R., Abrishamdari, M., & Mohammadi, M. H. P. (2017). Thin-Walled Structures Natural frequencies of functionally graded plates with porosities via a simple four variable plate theory: An analytical approach. *Thin Walled Structures, 120*(May), 366–377. https://doi.org/10.1016/j.tws.2017.08.003

Safaei, B., Ahmed, N. A., & Fattahi, A. M. (2019). Free vibration analysis of polyethylene/CNT plates. *European Physical Journal plus*. https://doi.org/10.1140/epjp/i2019-12650-x

Saidi, H., & Sahla, M. (2019). Vibration analysis of functionally graded plates with porosity composed of a mixture of Aluminum (Al) and Alumina (Al2O3) embedded in an elastic medium. *Frattura Ed Integrita Strutturale, 13*(50), 286–299. https://doi.org/10.3221/IGF-ESIS.50.24

Sayyad, A. S., Avhad, P. V., & Hadji, L. (2022). On the static deformation and frequency analysis of functionally graded porous circular beams. *Forces in Mechanics, 7*(March), 100093. https://doi.org/10.1016/j.finmec.2022.100093

Seçgin, A., & Sarigül, A. S. (2008). Free vibration analysis of symmetrically laminated thin composite plates by using discrete singular convolution (DSC) approach: Algorithm and verification. *Journal of Sound and Vibration, 315*(1–2), 197–211. https://doi.org/10.1016/j.jsv.2008.01.061

Shimpi, R. P. (2002). Refined plate theory and its variants. *AIAA Journal, 40*(1), 137–146. https://doi.org/10.2514/2.1622

Soleimanian, S., Davar, A., Eskandari Jam, J., Zamani, M. R., & Heydari Beni, M. (2020). Thermal buckling and thermal induced free vibration analysis of perforated composite plates: A mathematical model. *Mechanics of Advanced Composite Structures, 7*(1), 15–23. https://doi.org/10.22075/macs.2019.16556.1181

Van Vinh, P., & Huy, L. Q. (2022). Finite element analysis of functionally graded sandwich plates with porosity via a new hyperbolic shear deformation theory. *Defence Technology, 18*(3), 490–508. https://doi.org/10.1016/j.dt.2021.03.006

Verma, A. K., Kumhar, V., Verma, M., & Rastogi, V. (2022). Vibration analysis of partially cracked symmetric laminated composite plates using grey-taguchi. *Biointerface Research in Applied Chemistry, 12*(4), 4529–4543. https://doi.org/10.33263/BRIAC124.45294543

Wang, M., Xu, Y. G., Qiao, P., & Li, Z. M. (2019). A two-dimensional elasticity model for bending and free vibration analysis of laminated graphene-reinforced composite beams. *Composite Structures, 211*, 364–375. https://doi.org/10.1016/j.compstruct.2018.12.033

Xiang, S., & Wang, K. M. (2009). Free vibration analysis of symmetric laminated composite plates by trigonometric shear deformation theory and inverse multiquadric RBF. *Thin-Walled Structures, 47*(3), 304–310. https://doi.org/10.1016/j.tws.2008.07.007

Xue, Y., Jin, G., Ma, X., Chen, H., Ye, T., Chen, M., & Zhang, Y. (2019). Free vibration analysis of porous plates with porosity distributions in the thickness and in-plane directions using isogeometric approach. *International Journal of Mechanical Sciences, 152*(January), 346–362. https://doi.org/10.1016/j.ijmecsci.2019.01.004

Yüksel, Y. Z, & Akbaş, Ş. D. (2019). *Vibration analysis of a porous laminated composite plate*. I civilTech, Afyon Kocatepe University, pp. 1–10.

Zhang, Y. Q., Lu, Y., & Ma, G. W. (2008). Effect of compressive axial load on forced transverse vibrations of a double-beam system. *International Journal of Mechanical Sciences, 50*(2), 299–305. https://doi.org/10.1016/j.ijmecsci.2007.06.003

Zhang, Y., Shi, D., He, D., & Shao, D. (2021). Free Vibration Analysis of Laminated Composite Double-Plate Structure System with Elastic Constraints Based on Improved Fourier Series Method. *Shock and Vibration*. https://doi.org/10.1155/2021/8811747